

Growth and shape transformations of giant phospholipid vesicles upon interaction with an aqueous oleic acid suspension

Primož Peterlin^{a,*}, Vesna Arrigler^a, Ksenija Kogej^b, Saša Svetina^{a,c}, Peter Walde^d

^aUniversity of Ljubljana, Faculty of Medicine, Institute of Biophysics, Lipičeva 2, SI-1000 Ljubljana, Slovenia
^bUniversity of Ljubljana, Faculty of Chemistry and Chemical Technology, Aškerčeva 5, SI-1000 Ljubljana, Slovenia
^cJožef Stefan Institute, Jamova 39, SI-1000 Ljubljana, Slovenia
^dETH Zürich, Department of Materials, Wolfgang-Pauli-Str. 10, CH-8093 Zürich, Switzerland

Abstract

The interaction of two types of vesicle systems was investigated: micrometer-sized, giant unilamellar vesicles (GUVs) formed from 1-palmitoyl-2-oleoyl-*sn*-glycero-3-phosphocholine (POPC) and submicrometer-sized, large unilamellar vesicles (LUVs) formed from oleic acid and oleate, both in a buffered aqueous solution (pH = 8.8). Individual POPC GUVs were transferred with a micropipette into a suspension of oleic acid/oleate LUVs, and the shape changes of the GUVs were monitored using optical microscopy. The behavior of POPC GUVs upon transfer into a 0.8 mM suspension of oleic acid, in which oleic acid/oleate forms vesicular bilayer structures, was qualitatively different from the behavior upon transfer into a 0.3 mM suspension of oleic acid/oleate, in which oleic acid/oleate is predominantly present in the form of monomers and possibly non-vesicular aggregates. In both cases, changes in vesicle morphology were observed within tens of seconds after the transfer. After an initial increase of the vesicle cross-section, the vesicle started to evaginate, spawning dozens of satellite vesicles connected to the mother vesicle with narrow necks or tethers. In 60% of the cases of transfer into a 0.8 mM oleic acid suspension, the evagination process reversed and proceeded to the point where the membrane formed invaginations. In some of these cases, several consecutive transitions between invaginated and evaginated shapes were observed. In the remaining 40% of the cases of transfer into the 0.8 mM oleic acid suspension and in all cases of vesicle transfer into the 0.3 mM oleic acid suspension, no invaginations nor subsequent evaginations were observed. An interpretation of the observed vesicle shape transformation on the basis of the bilayer-couple model is proposed, which takes into account uptake of oleic acid/oleate molecules by the POPC vesicles, oleic acid flip-flop processes and transient pore formation.

Key words: giant vesicle, oleic acid, phosphatidylcholine, membrane growth

1. Introduction

The paper presents a study of the interaction between a micrometer-sized giant unilamellar vesicle (GUV) made from 1-palmitoyl-2-oleoyl-*sn*-glycero-3-phosphocholine (POPC) and a buffered (pH 8.8) suspension of oleic acid/oleate, consisting of either 100 nm large unilamellar vesicles (LUVs) at a concentration of oleic acid exceeding the critical concentration for vesicle formation (cvc), or predominantly monomers at concentrations below the cvc. The interaction was studied through the growth and the morphological shape changes of the POPC GUV, as visualized by an optical microscope.

Certain single-chain amphiphiles, *e.g.*, fatty acids with 10 carbon atoms or more, are known to form bilayers when their concentration is above the cvc, the temperature of the suspension is above the Krafft temperature (*i.e.*, the temperature at which their solubility equals the cvc), and its pH is above 7 [1, 2]. Their self-assembly differs from that of double-chain amphiphiles in a number of ways. On one hand, the cvc for single-chain amphiphiles is much higher ($\sim 10^{-3}$ – 10^{-4} M) than for

phospholipids (*e.g.*, the value for 1,2-dipalmitoyl-*sn*-glycero-3-phosphocholine (DPPC) is 4.6×10^{-10} M) [3]. On the other hand, unlike bilayers formed from phospholipids, which remain stable through a wide range of pH values, the type of aggregate formed by fatty acids in aqueous medium depends strongly on the pH of the medium, with two immiscible phases when the pH is clearly below the (apparent) acid dissociation constant ($\text{pH} \ll \text{pK}_a$), bilayers when $\text{pH} \sim \text{pK}_a$ and micelles when $\text{pH} \gg \text{pK}_a$.

A number of studies exists where similar interactions between phospholipid and oleic acid/oleate aggregates were studied on LUVs. It has been shown previously [4] that upon mixing POPC vesicles and oleic acid/oleate vesicles buffered to $\text{pH} \sim \text{pK}_a$, the oleic acid/oleate vesicles disappear, which has been explained by the dissociation of oleate from the oleic acid/oleate vesicles and its uptake by the phosphatidylcholine vesicles. In another experiment [5], a similar migration of fatty acid molecules from fatty acid vesicles to mixed phospholipid/fatty acid micelles has been observed. In suspensions of fatty acid vesicles at $\text{pH} \sim \text{pK}_a$, Luisi and co-workers as well as others [6, 7, 8] reported that the presence of existing oleic acid or phospholipid [9] vesicles catalyzed the spontaneous formation of oleic

*Corresponding author. Fax: +386-1-4315127.

Email addresses: primo.z.peterlin@m.f.uni-lj.si (Primož Peterlin)

acid vesicles resulting in newly formed vesicles that were more closely related in size to the pre-formed vesicles than to those formed spontaneously. Experiments with ferritin-labeled vesicles [10] indicated that the new vesicles formed via the process of increase of membrane area and fission of the preformed vesicles, rather than by being formed *de novo*. These experiments were conducted with large unilamellar vesicles, typically between 50 and 200 nm in size, and the observation relied on dynamic light scattering and electron microscopy [10, 11, 12]. The former method allows for monitoring the presence and/or size of vesicles/micelles in dependence on time, but does not provide a direct visual control, while the latter method offers a direct visual observation without the monitoring of the time dependence.

The work presented here tried to overcome the described limitations by studying the effects of fatty acid incorporation into phospholipid GUVs in a manner which allowed for a real-time visual monitoring using optical microscopy. In the experiments described, a single POPC GUV was transferred with a micropipette into a chamber filled with a suspension of oleic acid/oleate vesicles. For a comparison, a transfer into a suspension of oleic acid at a concentration lower than the cvc has also been performed.

The vesicle shape is a very sensitive indicator of the amount of oleic acid/oleate and/or phospholipid molecules in either leaflet of the bilayer, since the difference of the areas of the two membrane leaflets depends on them [13]. The occupancy of oleic acid/oleate molecules in either leaflet in turn depends on the balance between the rates of association, dissociation and translocation (flip-flop) of oleic acid molecules in the phospholipid membrane. Similar methodology – studying the effects of membrane modification through shape changes of phospholipid GUVs – has been used, for instance, in observations of chemically-induced shape transformations of GUVs [14], in experiments with lysolipids which intercalate into the phospholipid membrane [15, 16, 17], in the case when flippase activity was induced [18], in experiments where phospholipase A2 was microinjected onto or into individual vesicles, thus converting phospholipids into lysolipids [19], and for monitoring the effects of peptide incorporation into the phospholipid membrane [20, 21]. An important new feature of this study in relation to the ones mentioned above is that in the system studied here, during the course of the reaction, there is a much more significant increase of the membrane area due to the oleic acid/oleate incorporation into the membrane. Another important difference is that, unlike simple surfactants like lysolipids, which exist in either monomeric or micellar state, fatty acids can form bilayer structures.

2. Materials and methods

2.1. Materials

Oleic acid (*cis*-9-octadecenoic acid), D-(+)-glucose and D-(+)-sucrose were from Fluka (Buchs, Switzerland); Trizma base and Trizma HCl were from Sigma-Aldrich (St. Louis, MO, USA). 1-palmitoyl-2-oleoyl-*sn*-glycero-3-phosphocholine (POPC)

was purchased from Avanti Polar Lipids (Alabaster, AL, USA; purity > 99%, used without further purification). 2-(12-(7-nitrobenz-2-oxa-1,3-diazol-4-yl)amino)dodecanoyl-1-hexadecanoyl-*sn*-glycero-3-phosphocholine (NBD C₁₂-HPC) was purchased from Invitrogen (Eugene, OR, USA). Methanol and chloroform were purchased from Kemika (Zagreb, Croatia). All the solutions were prepared in doubly distilled and sterile water.

2.2. Preparation of giant lipid vesicles

Giant lipid vesicles were prepared from POPC using electroformation (a modified method of Angelova [22]) in 0.2 M sucrose and diluted with 0.2 M glucose, both buffered with 5 mM Trizma (pH 8.8). The lipids were dissolved in a mixture of chloroform/methanol (2:1, v/v) to a concentration of 1 mg/mL. 25 μ L of the lipid solution was spread onto two Pt electrodes and vacuum-dried for 2 hours. The electrodes were then placed into an electroformation chamber [23], which was filled with 0.2 M sucrose, buffered with 5 mM Trizma to pH 8.8. AC current (4 V/10 Hz) was then applied. After 2 hours the voltage and the frequency were reduced in steps, first to 3 V/5 Hz, after 15 minutes to 2 V/2.5 Hz, and after additional 15 minutes to the final values of 1 V/1 Hz, which were held for 30 minutes. The chamber was then drained and flushed with buffered 0.2 M glucose solution, yielding a suspension of GUVs in a 1:1 sucrose/glucose solution. The size distribution of the vesicles in the suspension was determined using dynamic light scattering on a 3D-DLS Research Lab (LS Instruments, Fribourg, Switzerland). Two samples were taken from a vial with a suspension of GUVs: one from the upper fraction, and another one from the bottom of the vial after the vesicles were left to settle for 30 minutes. Photon correlation spectroscopy showed that size distributions of both samples have a peak at 150 nm, the difference being that the bottom fraction contains a greater proportion of larger vesicles. As verified by optical microscopy, GUVs containing entrapped sucrose were mostly unilamellar and spherical, with diameters up to 100 μ m.

GUVs labeled with a fluorescent marker were prepared in a similar manner. First, NBD-labeled lipid was dissolved in chloroform/methanol (2:1, v/v) to a concentration of 1 mg/mL. Then, the solution of the NBD-labeled lipid in the chloroform/methanol mixture was added to a solution of lipid in the chloroform/methanol mixture in order to obtain either 1 or 2 wt% NBD-labeled lipid solution. The rest of the procedure for GUV preparation was the same as for the unmarked lipids.

2.3. Oleic acid suspensions

A suspension of large unilamellar vesicles (LUVs) from oleic acid/oleate was prepared using extrusion [24]. Oleic acid was dispersed in 0.2 M glucose solution with 5 mM Trizma buffer (pH 8.8) to a concentration of 50 mM. The suspension was stirred overnight with a magnetic stirrer bar before being diluted with 0.2 M glucose prepared with 5 mM Trizma buffer (pH 8.8) to the preferred concentration (0.3 mM or 0.8 mM). The rationale behind the choice of the oleic acid concentrations used is that the lower one is assumed to be below the cvc, and the higher one above it, as the cvc for oleic acid/oleate in the pH

range 8.5–9 is estimated to be around 0.4–0.7 mM [25], even though values as low as 0.082 mM [26] or as high as 1.0 mM [27] have been reported. The diluted suspension was subjected to 11 passes through two 100 nm polycarbonate membranes mounted in an Avestin LiposoFast extruder (Ottawa, Canada).

The osmolality of the suspension was determined by a Knauer automatic cryoscopic semi-micro osmometer (Berlin, Germany). The osmolality of 0.2 M buffered glucose solution was found to be 216 mOsm/kg and the osmolality of the suspension of 50 mM oleic acid in 0.2 M buffered glucose solution was found to be 207 mOsm/kg. As the suspension was diluted with buffered glucose solution before the experiment in a ratio 1:100 (v/v) or more, the difference between the osmolality of suspension and the osmolality of the buffered glucose solution was below the experimental error.

The size of oleic acid/oleate vesicles was determined using dynamic light scattering on a Malvern Zetasizer 3000 (Malvern Instruments, Malvern, UK). A 50 mM oleic acid/oleate suspension was prepared as described above. In order to achieve sufficient optical scattering signal, the suspension was extruded without dilution. A disposable cuvette was filled with approximately 2 ml of this suspension. Photon correlation spectroscopy showed that the distribution of oleic acid/oleate vesicle sizes (diameters) at pH 8.8 had a single peak at 69.1 ± 2.5 nm, with a polydispersity index [28] of 0.42 ± 0.14 .

2.4. Suspension of POPC LUVs

POPC LUVs were prepared using the freeze-thaw extrusion method. A round-bottomed flask was filled with 120.8 μL of 10 mg/mL POPC dissolved in a chloroform/methanol (2:1, v/v) mixture, to which 200 μL of chloroform was added. By turning the flask, chloroform evaporated and a lipid film was evenly distributed on the wall of the flask. Residual organic solvent was removed by drying at a reduced pressure (60 mmHg, water aspirator) for 2 h. The lipid film was then hydrated with 2.1 mL of 0.2 M glucose solution and vortexed using 250 μm glass beads. After six freeze-thaw cycles, 2 ml of the suspension was passed 11 times through two 100 nm polycarbonate membranes mounted in an Avestin LiposoFast extruder [24].

2.5. Microscopy and micromanipulation

The influence of aqueous suspensions of oleic acid on POPC GUVs was observed under an inverted optical microscope (Zeiss/Opton IM 35, objective Plan40/0.60 Ph2; Oberkochen, Germany) at 0.3 mM or 0.8 mM concentrations of oleic acid/oleate in the suspension. The micromanipulation chamber used had two compartments; one was filled with a suspension of POPC GUVs buffered to pH 8.8, the other (volume ≈ 250 μL) with an oleic acid/oleate suspension at a given oleic acid/oleate concentration, also buffered to pH 8.8. A spherical POPC GUV was selected, fully aspirated into a glass micropipette with a diameter exceeding the diameter of the vesicle, and transferred into the target suspension containing oleic acid, where the content of the micropipette was released (Fig. 1). After removing the micropipette, the vesicle was monitored and its shape changes were observed until the vesicle shape did not change any more.

The whole process was recorded with a Sony SSC-M370CE B/W video camera (Sony, Tokyo, Japan) and a Panasonic AG-7350 S-VHS video recorder (Matsushita Electric Industrial Co., Osaka, Japan). To allow for access with a micropipette, both compartments in a micromanipulation chamber were relatively thick (approximately 3 mm) and open on one side. An unwanted consequence of this was a constant convection flow in the chamber, both because of the evaporation and because of the heating due to the illumination light.

Fluorescent micrographs were obtained with an inverted optical microscope (Nikon Diaphot 200, objective Fluor 60/0.70 Ph3DM; Tokyo, Japan) with the epi-fluorescence attachment, micromanipulating equipment and a cooled digital camera (Hamamatsu ORCA-ER; C4742-95-12ERG; Hamamatsu, Japan), connected to a PC running Hamamatsu Wasabi software. The software also controlled a Uniblitz shutter (Vincent Associates, Rochester, NY, USA) in the light path of the Hg-arc light source. Micromanipulation chamber and the transfer procedure were identical in both setups.

Total internal reflection fluorescence microscopy was performed on an inverted optical microscope (Nikon Eclipse TE2000-E, objective Plan Apo TIRF 60/1.45 Oil) with an Ar-laser (488 nm; Melles Griot, Carlsbad, CA, USA) and a cooled digital camera (Nikon DS-2MBWc), connected to a PC running LIM Lucia G software (Laboratory Imaging, Prague, Czech Republic).

In the preparation procedure used, POPC vesicles in the glucose/sucrose solution mixture containing entrapped sucrose solution were transferred into an iso-osmolar glucose solution containing oleic acids. As the refractive index of a 0.2 M glucose solution ($n = 1.3316$, 26°C) differs from the refractive index of a 0.2 M sucrose solution ($n = 1.3355$, 26°C), the vesicle interior appears darker under a phase contrast microscope, and also exhibits a characteristic white halo around the vesicle. Refractive indexes of glucose and sucrose solutions were measured using an Abbe refractometer (Xintian WY1A, Guiyang, China).

2.6. Titration of a sodium oleate solution

A 20 mL sample of 10 mM oleic acid suspension in water was prepared and an equivalent amount of 1 M sodium hydroxide was added. 15 mL of this solution was transferred into a thermostated measuring cell. The oleate solution was titrated at 25°C with 0.1 M HCl in a nitrogen atmosphere under continuous stirring. The pH reached a constant value within ten minutes after the addition of each portion of the titrant. The pH was measured with an Iskra MA 5740 pH meter (Ljubljana, Slovenia).

2.7. Fluorescence spectrometry

Pyrene fluorescence emission spectra were recorded on a Perkin-Elmer LS-50 luminescence spectrometer (Norwalk, CT, USA) in a 10 mm quartz cuvette. The samples in concentration range from 0.1 to 1.5 mM of oleic acid were buffered to pH 8.7. Using excitation at 330 nm, the emission spectra of pyrene were recorded in the range from 350 to 550 nm. From

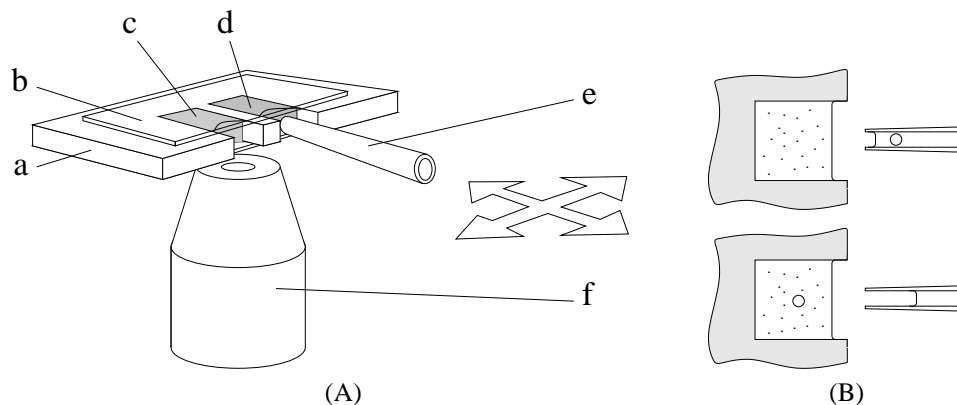


Figure 1: Micromanipulation setup for transferring POPC GUVs into a chamber with an oleic acid/oleate suspension (A). a – frame machined from 2 mm acrylic glass (polymethyl methacrylate, PMMA), mounted to the microscope stage; b – top 32 × 24 mm cover glass (an identical one is on the bottom side), mounted with a vacuum grease; c – chamber with the suspension of oleic acid/oleate LUVs; d – chamber with the suspension of POPC GUVs; e – micropipette mounted to the micromanipulator; f – microscope objective. B: Chamber c before (top) and immediately after (bottom) transfer of a POPC GUV. Schemes are not drawn to scale.

the spectra recorded at low oleic acid concentration, monomer peaks I_1 and I_3 were identified at 373 and 384 nm, respectively, while at higher concentrations of oleic acid, an additional broad excited-state dimer (excimer) peak I_E appeared at 473 nm, indicating formation of vesicles and/or micelles.

3. Results

3.1. General observations and classification of vesicle shape transformations

Under an inverted optical microscope, a single GUV prepared from POPC was transferred with a micropipette from a compartment with a POPC GUV suspension to a compartment with an oleic acid/oleate LUV suspension. A total of 54 vesicle transfers into a suspension containing 0.8 mM oleic acid and 9 transfers into a suspension containing 0.3 mM oleic acid were carried out and recorded on video.

The changes in the vesicle morphology served as a basis for the classification of the observations into groups. Immediately after the transfer into the oleic acid/oleate suspension, all vesicle transfer recordings exhibited a period in which the initial spherical shape of the selected vesicle did not change morphologically. This phase was followed by a phase of vesicle membrane evagination, where the vesicle spawned several “daughter” vesicles. Vesicles of the first group remained in this phase throughout the course of the observation. In the second group, the initial evagination was followed by an invagination, resulting in several invaginated vesicles within the “mother” vesicle. In the third group, such an invagination was followed by another evagination, forming several interconnected spherical vesicles or thick tubular structures. Denoting successive evaginations by E and invaginations by I, we classified the recorded vesicle transfers into five groups, from E to EIEIE. The sixth group comprises the transfers discarded due to various reasons (no visible changes; an abrupt vesicle rupture; the vesicle flew to a region where recording was no more possible). 13 out of 54 transfers into 0.8 mM oleic acid/oleate suspension and

class	sequence	# of instances	
		[oleic acid + oleate] 0.8 mM	0.3 mM
E	a	16	7
EI	a b	14	0
EIE	a b a	7	0
EIEI	a b a b	2	0
EIEIE	a b a b a	2	0

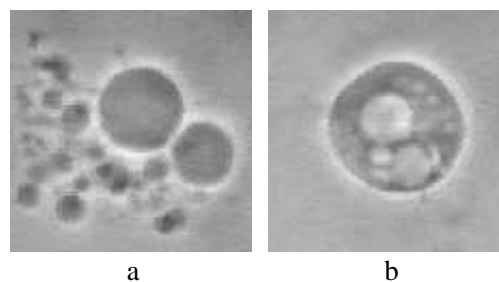


Figure 2: Classification of vesicle transfers with respect to the vesicle morphological changes in time course. Each group is labeled based on the sequence of evaginations (E) and invaginations (I) exhibited by the vesicle after the transfer into an oleic acid suspension, e.g., EI denotes a group of vesicle transfers which first exhibit vesicle evagination (a), being followed by an invagination of the vesicle (b). A sequence of morphological shapes with typical vesicle shape for each phase is shown for each vesicle class, along with the number of instances observed at either concentrations of oleic acid in the suspension (0.8 or 0.3 mM, pH 8.8).

2 out of 9 transfers into 0.3 mM oleic acid/oleate suspension were discarded due to the problems described. Fig. 2 shows the classification of the vesicle recordings into groups and indicates the frequency of observations, together with examples of evaginated and invaginated shapes. No statistically convincing relationship has been found between the class of the vesicle transfer and any measurable parameter. Possible influences include the volume and the area-to-volume ratio of the GUV, local variations in the temperature, pH, and the convective flow in the chamber, as well as the effects of micropipette manipulation during the transfer. The recording was terminated when either the morphological changes apparently stopped, or the changes were too slow to justify continuing recording.

During the course of the experiment, no significant change in the contrast between the GUV interior and exterior was observed, *i.e.*, throughout the experiment, the vesicle interior appeared equally darker than the surrounding medium. This indicates that the amount of sucrose inside the vesicle which exchanged with the glucose in the environment was below the detection level of our setup. Since the osmotic conditions remained unchanged, we can assume that the volume of the GUV remained constant as well.

In several cases, the evaginations, which appeared upon the transfer of a POPC GUV to either a 0.3 mM or a 0.8 mM suspension of oleic acid/oleate, were in the form of thin tubular protrusions or tethers. In order to test the presence of phospholipid in the thin tubular protrusions, we conducted an experiment where POPC was marked with 2% NBD-labeled lipid. We noticed fluorescence both in the tubular protrusions and in the vesicle bodies (Fig. 3), and on the basis of the evidence that the calculated diffusion rates for NBD-labelled phospholipids [29] are comparable with the results for POPC [30] (both $D \sim 10^{-11} \text{ m}^2/\text{s}$), it is reasonable to expect that apart from NBD-PC, some unlabelled POPC may also be present in the tubular protrusions.

3.2. Control experiments

The pH region where oleic acid/oleate at a total concentration of 9.9 mM forms bilayer structures was determined by titration. The titration was started with a 9.9 mM suspension of oleic acid prepared in a 9.9 mM aqueous solution of NaOH, thus deprotonating the COOH groups of oleic acid. 100 mM HCl was then added stepwise and the pH was measured. Fig. 4 shows the resulting titration curve, which is in agreement with previously published results obtained under similar experimental conditions [31, 32, 33] and indicates that bilayer structures are present in the pH region from 8.4 to 10.2, while above pH 10.2, only micelles exist, as indicated by the optical transparency of the corresponding solutions.

The presence of oleic acid/oleate aggregates was determined using pyrene fluorescence emission spectrometry. It is known [34, 35] that pyrene is preferentially solubilized in the hydrophobic environment of surfactant aggregates, *i.e.*, in the bilayer or micelle cores. Fig. 5a displays the fluorescence emission spectrum, showing that below the cvc of oleic acid/oleate (0.4–0.7 mM, [25]), only pyrene monomer peaks were present, while

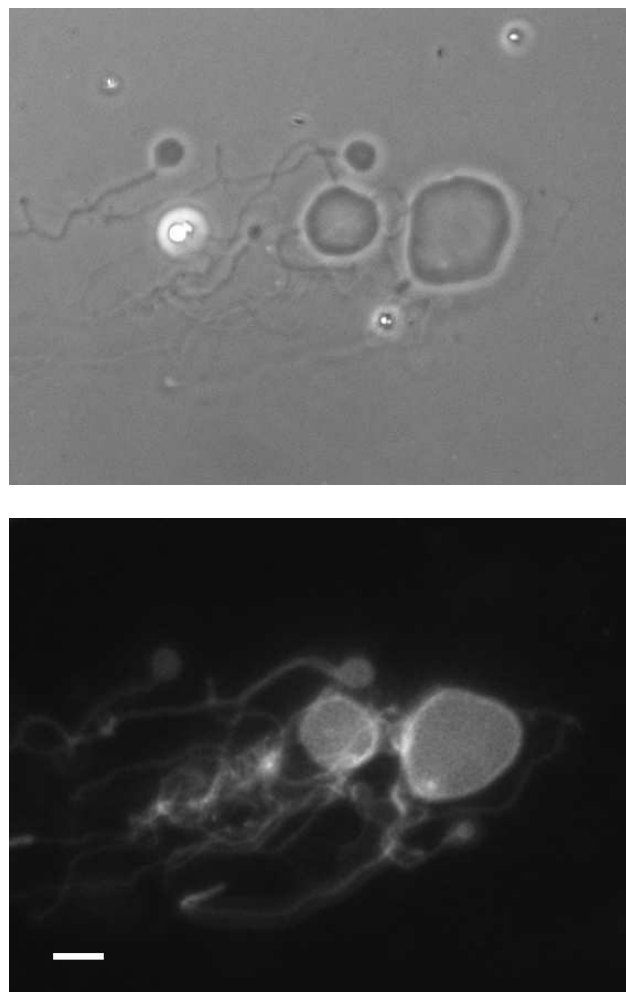


Figure 3: Top: a POPC GUV with 2% NBD-labeled lipid shown approximately 3 min after the transfer into a 0.8 mM suspension of oleic acid/oleate in 0.2 M glucose (pH 8.8), shown with the phase contrast technique. Bottom: a fluorescent image of the same vesicle. The bar in the bottom frame represents 10 μm .

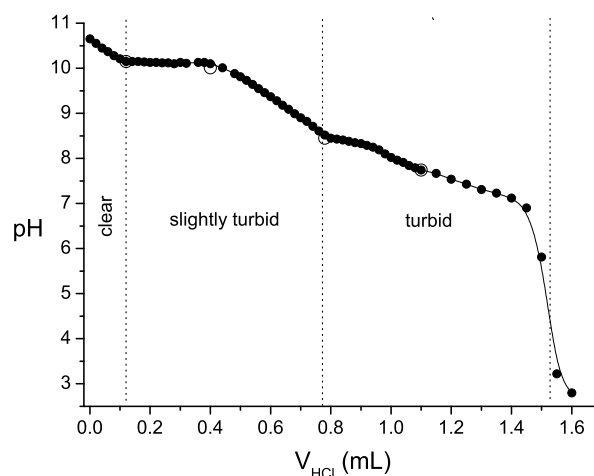
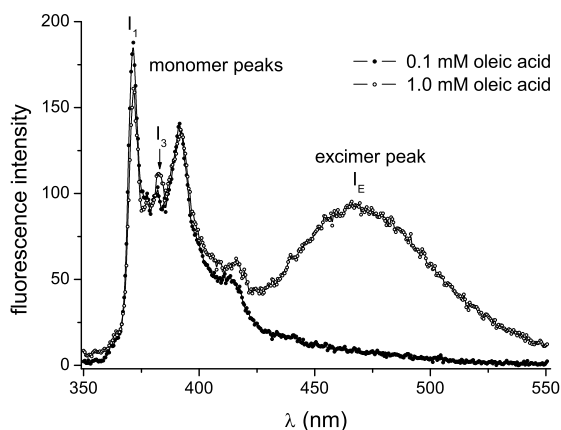
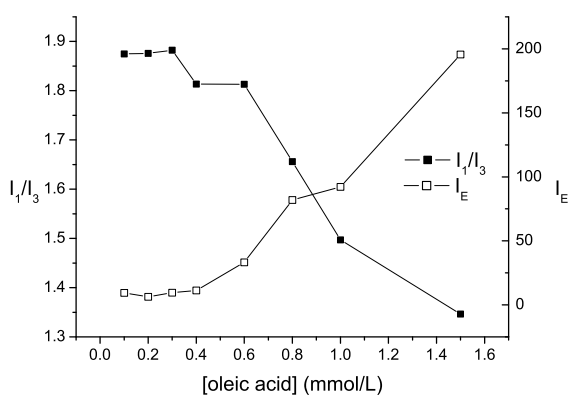


Figure 4: Equilibrium titration curve of 9.9 mM oleic acid/oleate (15 mL) determined with 0.1 M HCl at 25°C.



(a)



(b)

Figure 5: (a) Pyrene emission fluorescence spectra of 0.1 mM oleic acid (\circ) and 1.0 mM oleic acid (\bullet) buffered to pH 8.7. Below the cvc, only monomer peaks are present, while above the cvc, a broad excimer peak appears. (b) The intensity ratio of the monomer emission peaks I_1/I_3 and the intensity of the pyrene excimer peak (I_E ; determined at 473 nm) as a function of oleic acid concentration, buffered to pH 8.7.

a broad excimer peak appeared above the cvc, which is consistent with published results [36]. The ratio of the two monomer peaks, I_1/I_3 , indicates whether pyrene molecules are enclosed in a polar or a non-polar environment: high values (1.7 or above) indicate that pyrene is in a highly polar environment (*e.g.*, water), while low values (1.3 or below) indicate a non-polar environment [37]. Fig. 5b shows the I_1/I_3 ratio and the height of the pyrene excimer peak I_E , determined at 473 nm, as a function of the concentration of oleic acid/oleate in suspension at pH 8.7. A simultaneous drop of I_1/I_3 and an increase of I_E around 0.6 mM oleic acid in Fig. 5b indicates that a non-polar environment started to be formed at this concentration. This value is consistent with some of the estimates for the cvc in this pH range [25].

In order to determine whether the presence of oleic acid/oleate molecules is necessary for the observed shape changes, POPC GUVs were transferred into a solution of glucose, buffered to pH 8.8 with Trizma. In 5 recorded vesicle transfers, no shape

changes were observed. Furthermore, if POPC GUVs were transferred into a suspension of POPC LUVs in an iso-osmolar glucose solution, no shape changes occurred (8 recorded vesicle transfers). This is in agreement with the previous findings [4] and clearly shows that the shape changes are related to the presence of oleic acid/oleate.

In an attempt to explain the consecutive transitions between an evaginated and an invaginated shape, we wanted to exclude the possibility that the evagination-to-invagination transition is a simple effect of losing lipids from the outer membrane layer due to adhesion of the membrane to the glass surface (the vesicles were in contact with the bottom of the observation chamber, because they were filled with a solution with a density greater than the density of the environment). In the experiment carried out, the POPC vesicle membrane was marked with 1% NBD-labeled lipid, and evidence for lost patches of membrane during the vesicle movement over the surface due to the convective flow was sought utilizing total-internal-reflection fluorescence (TIRF) microscopy. No evidence of lost patches of lipid was found.

3.3. Time course of a typical vesicle transfer

Several characteristic events and selected stages of vesicle development will be illustrated in the case of a single vesicle transfer (Fig. 6 and a movie; see Supplementary data). A 17 minutes long recording of a transfer of a vesicle from the group EIE was selected as an example.

The increase of vesicle cross-section followed a characteristic pattern (Fig. 6a and movie, 01:00 to 01:28 (Supplementary data); Fig. 7). First, the vesicle sunk to the bottom of the observation chamber within approximately 10 s. The sinking of the vesicle was verified by the necessary manipulation of the microscope z -axis to keep the vesicle in focus, as well as by the noticed decrease or even cessation of vesicle drift. During the time of sinking, as well as throughout a certain period after the vesicle sunk to the bottom, the vesicle cross-section remained spherical and its radius remained constant. This phase was followed by a phase when the vesicle cross-section was increasing at an approximately constant rate while maintaining axial symmetry with respect to the normal to the chamber bottom.

The phase of gradual increase of the vesicle cross-section was terminated by an abrupt symmetry-breaking transition (Fig. 6b and movie, 01:33 to 01:38, Supplementary data), where the vesicle spawned several daughter vesicles on the timescale of seconds. After this initial outburst, new daughter vesicles were spawned one by one at an approximately constant rate. Fig. 6c (movie 01:55 to 02:13, Supplementary data) shows two events when consecutive buds were forming in a short time span on the same membrane section. New daughter vesicles were formed on the surface of the “mother” vesicle, while the existing daughter vesicles were not affected. It is worth noting that the buds were approximately of the same size. As it became evident in the further development, all daughter vesicles remained connected to the mother vesicle with narrow necks or tethers.

After persisting in an evaginated shape for approximately 50 s, the membrane abruptly started to invaginate (Fig. 6d and movie, 02:16 to 02:44, Supplementary data). The complete

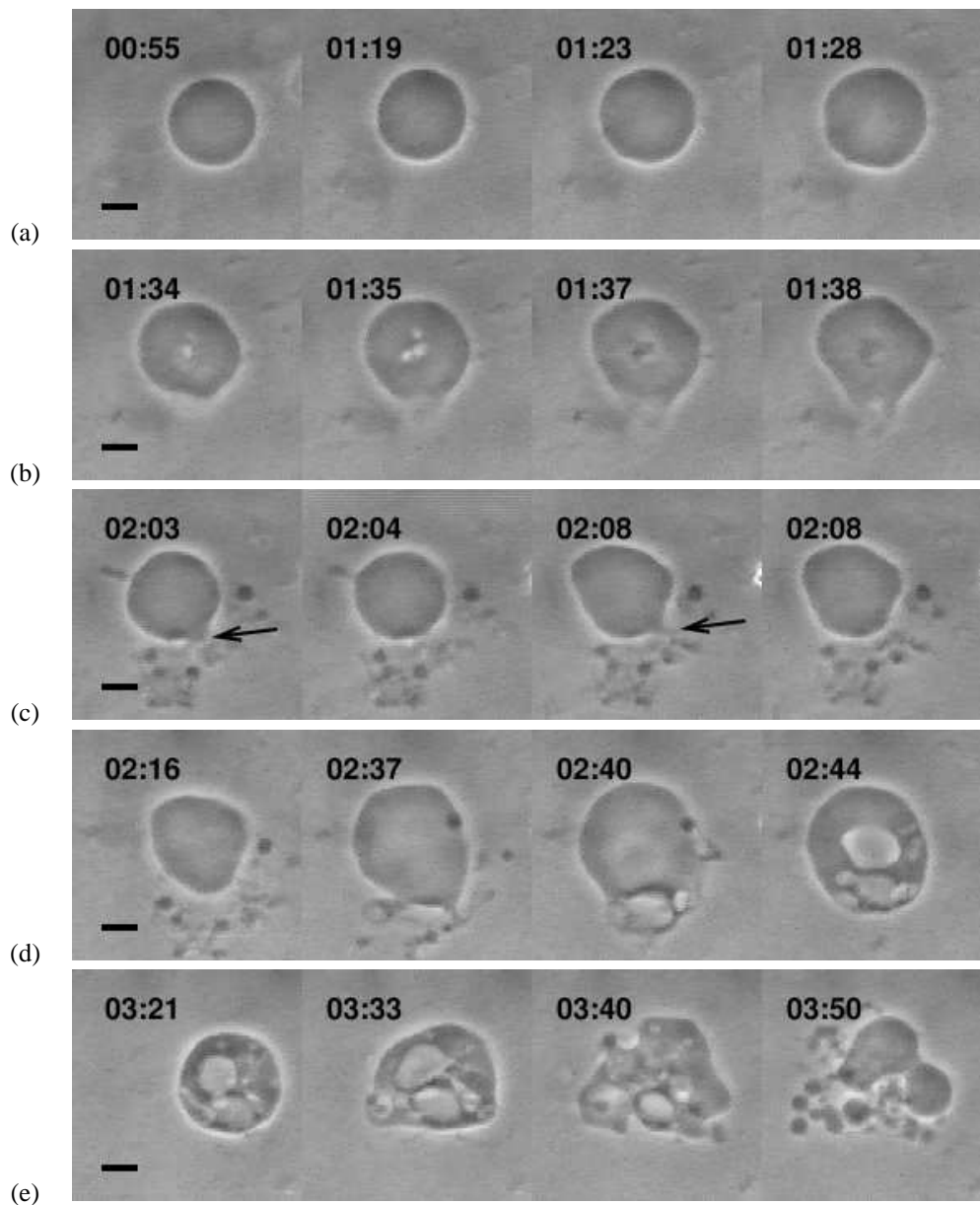


Figure 6: Characteristic events in the course of shape transitions of a POPC GUV upon the transfer into 0.8 mM suspension of oleic acid in 0.2 M glucose. (a) Initial increase of the vesicle cross-section. (b) An abrupt shape transition. (c) Vesicle budding (buds forming indicated by arrows). Two buds formed from a series of four consecutive buds are shown. (d) An invagination process. (e) An evagination process. The bar in the leftmost frame of each strip represents $10\ \mu\text{m}$. Time marks denote the time since the transfer.

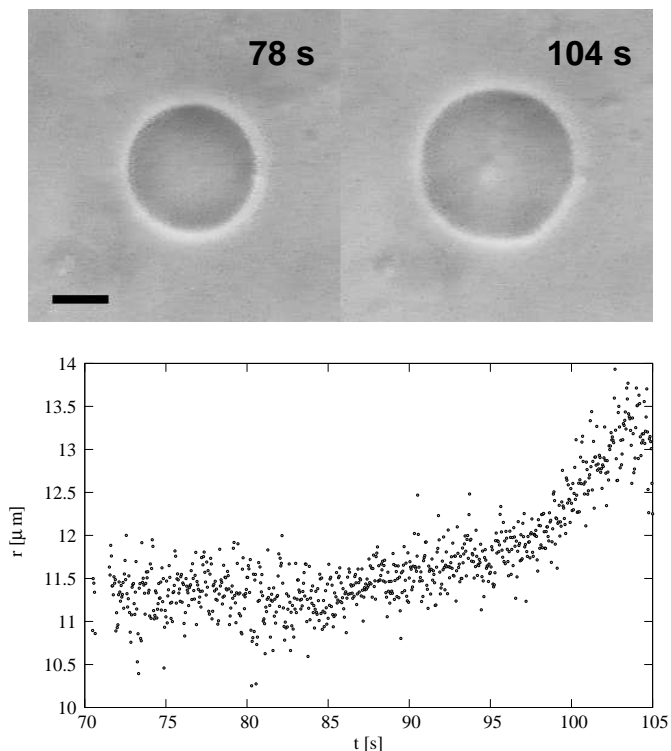


Figure 7: Top: a POPC GUV shown 78 s after the transfer into a 0.8 mM suspension of oleic acid in 0.2 M glucose (left), and 104 s after the transfer (right). The bar in the left frame represents 10 μm . Bottom: vesicle radius as a function of the time elapsed after the transfer.

transition lasted approximately 20 s. Invaginations often started at the tip of the protrusions, which were then retracted into the vesicle body (Fig. 8).

This invaginated phase ended after approximately 40 s, when the membrane started to evaginate again (Fig. 6e and movie, 03:20 to 03:50, Supplementary data). The transition was completed in approximately 25 s. Afterwards, the vesicle remained in an evaginated shape without qualitative changes of shape for the next 13 minutes (movie, 3:50–16:40, Supplementary data), after which the recording was terminated.

4. Discussion

Although comparable earlier investigations performed on POPC LUVs offer ample evidence that the oleic acid molecules are taken up by the phospholipid vesicles, leading to their growth and eventually – depending on the experimental conditions – to vesicle fission [9, 10, 11, 12], no direct real-time visualization of the process has been reported so far. In this work, instead of POPC LUVs, we used POPC GUVs since they allow a direct observation by light microscopy and made some novel and unexpected observations during the course of our investigations. It is the purpose of this discussion to offer a possible qualitative explanation of the mechanisms underlying the observed phenomena: the increase of the membrane area, the transient increase of the difference of the areas of the outer and the inner membrane leaflet, and the oscillations of the latter. The sec-

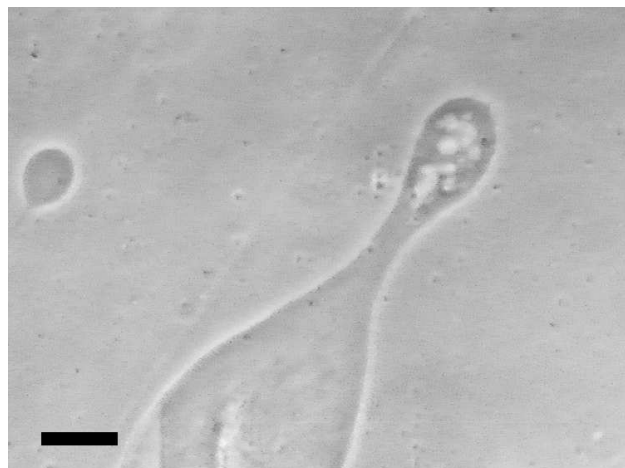


Figure 8: Invaginations start at the tip of protrusion, when the protrusion is retracting into the vesicle body. Image recorded 2 min 7 s upon the transfer of a POPC GUV into a 0.8 mM suspension of oleic acid in a 0.2 M sucrose/glucose solution buffered to pH 8.8. The bar represents 20 μm .

tion concludes by indicating open issues, which require further work.

4.1. Increase of membrane area

Membrane area significantly increases. On two occasions in the course of the experiment, an increase of the membrane area can be demonstrated. Shortly after the transfer, when the POPC vesicle geometry is still simple, it is possible to estimate its area with an accuracy of a few percent. Towards the end of the experiment, when the dynamics of the shape changes subsides, a more crude estimate is possible.

The results plotted in Fig. 7 show that the diameter of the cross-section of an approximately spherical GUV initially remained constant after it sank to the bottom of the observation chamber with oleic acid/oleate suspension, and then increased by about 15%. Approximating the transformation with a change from a sphere to an oblate spheroid with a volume equal to the volume of the sphere, one can estimate that a 15% increase of the diameter of the vesicle cross-section amounts to an approximately 3% increase of the membrane area at this stage of the oleic acid/oleate intercalation, which corresponds to oleic acid/oleate representing $\sim 4\text{--}5$ mol % in the membrane composition. Flaccid vesicles filled with a solution which exceeds in density the external solution are known to deform into approximately oblate spheroids also due to gravity [38]. However, the observed extent of deformation can not be explained by gravitation alone.

The complex vesicle geometry towards the end of the experiment only allows for a very rough quantification. We estimate that the final membrane area can be as large as five times its initial value, which corresponds to oleic acid/oleate representing up to ~ 85 mol % of the membrane composition. Vesicle shapes seem to reach an equilibrium in the conditions of excess oleic acid/oleate: the amount of oleic acid/oleate available in the chamber is $\sim 10^{17}$ molecules, and thus vastly exceeds the amount of phospholipid: a 10 μm GUV contains $\sim 4 \times 10^9$

molecules, and even if 10- or 100-times as much lipid is unintentionally introduced into the chamber with a micropipette transfer, the ratio is still in the order of $\sim 1 : 10^6$.¹ A significant increase of membrane area is in agreement with previous experiments on POPC LUVs [9, 10, 11].

Membrane area growth can be related to system kinetics. In a simple kinetic scheme describing the kinetics of the interaction of fatty acids with phospholipid membranes [40], the system is represented by the populations of oleic acid/oleate molecules in the following four compartments: the vesicle exterior, the outer membrane leaflet, the inner membrane leaflet, and the vesicle interior. Two of these, the populations of oleic acid in both membrane leaflets are directly related to the equilibrium areas of the outer (A_{20}) and the inner (A_{10}) membrane leaflet.² Both A_{20} and A_{10} vary with time due to three processes: (i) association of fatty acid molecules with the phospholipid membrane, where the rate of the membrane area increase is proportional to the concentration of oleic acid/oleate in the membrane vicinity and the area available for intercalation; (ii) dissociation of fatty acid molecules from the phospholipid membrane, its rate being proportional to the oleic acid population in the membrane leaflet, and (iii) fatty acid translocation (flip-flop) in the membrane, its net flow being proportional to the difference of oleic acid populations in the two leaflets. Fatty acid association and dissociation occur both on the external and the internal membrane-water boundary. The association of oleic acid monomers to a phosphatidylcholine membrane is considered to be a very fast process [41, 42], while the question whether the oleic acid translocation is faster [43, 44] or slower [41, 45] than the dissociation appears to be an unresolved question.

The demonstrated increase of the membrane area requires that the areas of both membrane leaflets must increase, implying that by some means, translocation of oleic acid must have occurred. Furthermore, the transitions cease once the oleic acid/oleate in the suspension is in equilibrium with the oleic acid/oleate in the membrane on both the internal and the external side of the membrane. This implies that the concentration of oleic acid/oleate in the vesicle lumen is equal to the external concentration, and that both the translocation and dissociation must have occurred within the observed timescale.

4.2. Transient increase of the difference between the areas of the outer and the inner membrane leaflet

Shape changes commence with an evagination. In all 48 observed cases of POPC GUV transfer into a suspension of oleic acid/oleate, its concentration being either above or below the

¹It is assumed in the estimate that the average headgroup area of a phospholipid molecule is $a_0 \approx 60 \text{ \AA}^2$ [39, Ch. 3] and that the vesicles are unilamellar; therefore a GUV with a radius r contains $N_{\text{PC}} \approx 2 \times 4\pi r^2 / a_0$ molecules.

²We have used the index "0" to denote the equilibrium values of the area of a membrane leaflet, as opposed to their instantaneous values A_2 and A_1 . The latter may differ from their equilibrium values: *e.g.*, intercalation of molecules into the outer membrane leaflet, as in the experiment described, induces lateral tension in both membrane layers, the outer one being compressed and the inner one stretched.

cvc, shape transformations always commenced with a transition into an evaginated shape. In 16 out of 41 cases where the concentration of oleic acid/oleate in the suspension was above cvc and in all 7 observed cases where the concentration of oleic acid/oleate in the suspension was below the cvc, vesicle persisted in this shape until the end of the experiment.

The relation with the bilayer couple model. Vesicle shape can be related to the difference between the areas of the outer and the inner membrane leaflet $\Delta A_0 = A_{20} - A_{10}$ [46]. Given the values of $A_0 = 2A_{10}A_{20}/(A_{10} + A_{20})$ and ΔA_0 , a vesicle adapts its shape (along with A and ΔA , which correspond to a given shape) in order to minimize its total energy, comprising of membrane stretching and membrane bending energy [47], as well as the entropic free energy contribution due to thermal fluctuations [48]. Shapes with ΔA_0 larger than the value of ΔA_0 for a sphere are evaginated, and those smaller are invaginated. At values of ΔA_0 which significantly exceed the value of ΔA_0 for a sphere, it is expected that vesicle shapes look like the so-called limiting shapes, *i.e.*, shapes with a maximal volume at given A and ΔA , which were shown to consist of connected spheres of two allowed sizes [13, 49, 50]. The observed (quasi-)equilibrium shapes were one or a few bigger spheres connected to numerous smaller spheres, which approximately agrees with the bilayer couple model. This state may superficially resemble vesicle growth and fission observed in the experiments with LUVs (*e.g.*, [6, 9, 11, 12]), however, we need to emphasize that in our case the newly formed daughter vesicles remained tethered to the mother vesicle, *i.e.*, no real separation of membrane into two entities has been observed.

The effect of oleic acid intercalation on spontaneous curvature. Apart from affecting A_0 and ΔA_0 , the intercalation of oleic acid molecules into POPC membrane changes its composition. This could also affect its spontaneous curvature [47], since the spontaneous curvature depends on the shapes of the membrane constituents. POPC molecules are approximately cylinder-shaped, which makes their intrinsic curvature close to zero, favoring their aggregation into flat bilayer structures [51]. Protonated oleic acid molecules have a slightly negative intrinsic curvature [52], while deprotonated oleic acid molecules, *i.e.*, oleate ions, exert mutual electrostatic repulsion between their headgroups, which favors their aggregation into micelles or other structures with highly positive curvature. At $\text{pH} \sim \text{pK}_a$, where approximately half of the oleic acid molecules are protonated, it is known that the aggregates formed by oleic acid/oleate molecules are bilayers. If one assumes a similar behavior in mixed phospholipid/oleic acid/oleate bilayers, the average spontaneous curvature of a membrane composed of phospholipid, and equal amounts of oleic acid and oleate is expected to be close to zero. We can therefore conclude that in the conditions the experiment was conducted, *i.e.*, at $\text{pH} \sim \text{pK}_a$, oleic acid/oleate forms bilayer structures with zero intrinsic curvature, and the effect of oleic acid intercalation into the membrane onto the spontaneous curvature is minor in comparison to its effect on ΔA_0 .

Consecutive vesicle budding. On several occasions, usually later in the course of morphological changes caused by the incorpo-

ration of oleic acid into the membrane, we noticed several consecutive buds being formed on the same membrane section in a short time span (Fig. 6c; movie 01:55 to 02:13, see Supplementary data). Such a process, which lasted for a certain period of time, means that during this period, ΔA_0 and A_0 were increasing in the appropriate ratio. Such processes have not been observed in the experiments with lysolipids [15, 53], because in the latter case, no significant change of A_0 has been noticed. It is worth noting that the buds were usually found to be of approximately the same size, which is a confirmation that the vesicle shape belongs to limiting shapes. The budding is also an important mechanism in the processes of membrane trafficking, *e.g.*, in the endoplasmatic reticulum and endocytosis. The studies of budding in cells indicate that this process can only occur with the support of a complex protein network [54]. The observed consecutive formation of buds during a certain period of time demonstrates that budding can also occur as a simple physical reaction of membrane to a simultaneous increase in both the total membrane area and the difference in the outer and the inner leaflet area.

4.3. Oscillations of ΔA

Non-specific convective flow. In 25 out of 41 cases of vesicle transfer into a suspension where the concentration of oleic acid/oleate is above *cvc*, the initial membrane evagination has been followed by a membrane evagination. Such shape changes correspond to a decrease of ΔA from a value larger to a value smaller than the value of ΔA for a sphere. This phenomenon can not be explained with a simple kinetic model mentioned above. In addition to oleic acid association, dissociation and diffusive translocation, we propose another non-specific mechanism for translocation, which employs membrane defects or pores that occur stochastically [55, 56]. In the initial stage shortly after the transfer of GUV, oleic acid intercalation into the outer membrane leaflet leads to the overpopulation of the outer membrane leaflet with respect to the inner one, and consequently to an imbalance in lateral tensions of the two membrane leaflets. The two membrane leaflets tend to relax, and when a membrane defect occurs, the difference in lateral tensions causes a convective flow of membrane components from the outer to the inner leaflet. It is to be noted that all species of molecules – phospholipid, oleic acid and oleate ions – can traverse the membrane via the convective flow, their ratios in the flow being proportional to their ratios in the outer membrane leaflet. Via this mechanism, the population of phospholipid in the inner membrane leaflet exceeds its population in the outer membrane leaflet. At this point, phospholipids alone would favour invaginated shape; however, due to the influx of oleic acid/oleate into the outer membrane leaflet, the overall shape is still evaginated. As the diffusive flip-flop rate for oleic acid is much higher than the corresponding flip-flop rate for phospholipids [57, 58], at some point both the concentration of oleic acid/oleate in the vesicle lumen equilibrates with the external concentration, and the population of oleic acid/oleate in the inner membrane leaflet equilibrates with the one in the outer membrane leaflet. A low flip-flop rate for phospholipids together with virtually no net convective flow, since there is no

imbalance in lateral tensions of the two membrane layers either, means that this quasi-equilibrium state is a kinetic trap for the phospholipid. With oleic acid in balance, the vesicle shape is determined by the populations of phospholipid in the two membrane leaflets, which favour an invaginated shape. Note that the vesicle interior is osmotically balanced with the exterior throughout the experiment, so no net flux of water is expected to occur through these pores. We can thus conclude that the observed shape transition from evaginated to invaginated shapes can be explained, if one allows for a non-specific convective flow through stochastically occurring membrane defects [56].

4.4. Open issues

A burst of satellite vesicles vs. a gradual increase in their number. In the experiments carried out, we observed an abrupt transition, where GUV persisted in an approximately oblate shape for a certain period of time, this being followed by sprouting a number of satellite vesicles in a short period of time. This is seemingly in contradiction with the bilayer-couple theory, which predicts a gradual one-by-one increase as the ΔA_0 increases. The explanation for this absence of intermediate steps possibly involves the entropic contribution due to thermal fluctuations [48], which lowers the free energy of a fluctuating oblate spheroid below the free energy of a spherical vesicle with spherical satellites.

The satellite spheres were not all exactly the same size. The observed state with a few larger vesicles and several smaller satellite vesicles of approximately the same size is consistent with the notion of the bilayer-couple model. However, the satellite vesicles observed in the experiment were not exactly of the same size, and there are several possible reasons for that: (a) the model is valid for an equilibrium system, while the observed system might not have reached the equilibrium yet, (b) the model is valid for a homogenous membrane, while the mixed phospholipid/oleic acid membrane is not necessarily laterally homogeneous, and (c) satellite vesicles formed at different times are also formed at slightly different conditions (*e.g.*, the composition of membrane changes); however, once formed, they are found in a kinetic trap, as the energy needed to reopen and close the neck connecting two spheres far exceeds the energy difference between different configurations.

Higher oscillations. We observed a comparably frequent (11 out of 41 cases) shape transitions from invaginated shape back into evaginated shape, and in a few cases even higher oscillations (Fig. 2). Although it remains to be seen whether the convective-flow mechanism described above can reproduce such behaviour with realistic values of parameters, we would not want to exclude the possibility that another mechanism is in effect, possibly connected to spatial inhomogeneity of oleic acid/oleate concentration.

Direct interaction with oleic acid/oleate aggregates. A qualitative difference between the GUV behaviour in the cases where the concentration of oleic acid/oleate in the suspension was below *cvc*, and the cases where its concentration was above *cvc*,

i.e., where oleic acid aggregates were present, opens a possibility that another interaction pathway was present in the latter case. While the prevalent opinion seems to be that the oleic acid/oleate monomers dissociate from the donor system before being incorporated in the phospholipid membrane (*e.g.*, [40]), some authors allow for a possibility that oleic acid/oleate aggregated intermediates directly interact with a phospholipid membrane [36]. The two proposed pathways differ in their effect on the vesicle shape. While the interaction with monomers directly increases the area of the outer membrane leaflet and only indirectly, through translocation, the area of the inner membrane leaflet, a possible interaction with an aggregated intermediate would contribute to both membrane leaflets at the same time. However, since LUVs have a large intrinsic ΔA_0 , both mechanisms are expected to result in a shape evagination, and the experiment we conducted can not be used to distinguish between the two.

Oleic acid flip-flop: fast or slow? There is an ongoing debate whether the oleic acid translocation is fast or slow. The results obtained with free fatty acids [43, 44] yield much higher rates than those obtained with BSA-complexed fatty acids [41, 45]. It has been suggested [42] that exposure to fatty acid concentrations higher than $5 \mu\text{M}$ somehow perturbs the bilayer structure, which may result in a higher apparent translocation rate. We would like to emphasize that the two mechanisms for oleic acid/phospholipid translocation proposed in this paper – diffusive flip-flop and non-specific convective flow – work in a similar way. At very low concentration of oleic acid/oleate in the suspension, there is virtually no imbalance in lateral tensions of the two membrane layers, and the outward and the inward convective flows are balanced, thus the only mechanism for oleic acid translocation is diffusive flip-flop, driven by the imbalance in oleic acid concentration. At higher concentrations, however, convective flow, driven by the imbalance in lateral tensions, opens another, possibly faster, pathway. Although this complex issue is probably far from being resolved, we hope this notion may help by providing another viewpoint to this seemingly conflicting issue.

5. Conclusions

By working with GUVs in the optical microscopy regime, this study offers a new insight into the budding process by which new daughter vesicles can be formed from phospholipid vesicles by virtue of the incorporation of fatty acids into the phospholipid membrane. These observations complement previous findings obtained by other methods, which showed an increase of the number of LUVs upon the transfer into an oleic acid/oleate suspension [12]. We offer a qualitative explanation of the observed phenomena, however, further work in the direction of the determination of kinetic and mechanical properties of this system and building the corresponding theoretical model will be needed for its confirmation. The observed budding and formation of satellite vesicles induced solely by a membrane growth without the intervention of proteins may have an implication for

the understanding of the basic principles governing membrane trafficking.

Acknowledgments

The authors would like to thank Dr. Bojan Božič, Dr. Martin Hanczyc, Dr. Janja Majhenc, and Dr. Andrea Parmeggiani for their valuable discussions and suggestions. Dr. Pegi Ahlin Grabnar performed the photon correlation spectroscopy of oleic acid/oleate vesicles, and Miha Šušteršič helped with the vesicle classification. This work has been supported by the Slovenian Research Agency research grant P1-0055 and the COST Action D27.

Supplementary data

An annotated video recording from which the strips in Fig. 6 were selected is available as an online supplement. This information is available via the Internet at <http://biofiz.mf.uni-lj.si/~peterlin/su>

References

- [1] J. M. Gebicki, M. Hicks, Preparation and properties of vesicles enclosed by fatty-acid membranes, *Chem. Phys. Lipids* 16 (2) (1976) 142–150.
- [2] W. R. Hargreaves, D. W. Deamer, Liposomes from ionic, single-chain amphiphiles, *Biochemistry* 17 (18) (1978) 3759–3768.
- [3] R. Smith, C. Tanford, Critical micelle concentration of L- α -dipalmitoylphosphatidylcholine in water and water/methanol solutions, *J. Mol. Biol.* 67 (1972) 75–83.
- [4] Z. Cheng, P. L. Luisi, Coexistence and mutual competition of vesicles with different size distributions, *J. Phys. Chem. B* 107 (2003) 10940–10945.
- [5] S. M. Fujikawa, I. A. Chen, J. W. Szostak, Shrink-wrap vesicles, *Langmuir* 21 (2005) 12124–12129.
- [6] E. Blöchliger, M. Blocher, P. Walde, P. L. Luisi, Matrix effect in the size distribution of fatty acid vesicles, *J. Phys. Chem. B* 102 (1998) 10383–10390.
- [7] M. Hanczyc, J. W. Szostak, Replicating vesicles as models of primitive cell growth and division, *Curr. Opin. Chem. Biol.* 8 (2004) 660–664.
- [8] S. Chungcharoenwattana, H. Kashiwagi, M. Ueno, Effect of preformed egg phosphatidylcholine vesicles on spontaneous vesiculation of oleate micelles, *Colloid Polym. Sci.* 283 (2005) 1180–1189.
- [9] S. Lonchin, P. L. Luisi, P. Walde, B. H. Robinson, A matrix effect in mixed phospholipid/fatty acid vesicle formation, *J. Phys. Chem. B* 103 (1999) 10910–10916.
- [10] N. Berclaz, M. Müller, P. Walde, P. L. Luisi, Growth and transformation of vesicles studied by ferritin labelling and cryotransmission electron microscopy, *J. Phys. Chem. B* 105 (2001) 1056–1064.
- [11] N. Berclaz, E. Blöchliger, M. Müller, P. L. Luisi, Matrix effect of vesicle formation as investigated by cryotransmission electron microscopy, *J. Phys. Chem. B* 105 (2001) 1065–1071.
- [12] P. Stano, E. Wehrli, P. L. Luisi, Insights into the self-reproduction of oleate vesicles, *J. Phys.: Condens. Matter* 18 (33) (2006) S2231–S2238.
- [13] S. Svetina, B. Žekš, Membrane bending energy and shape determination of phospholipid vesicles and red blood cells, *Eur. Biophys. J.* 17 (1989) 101–111.
- [14] F. M. Menger, N. Balachander, Chemically-induced aggregation, budding and fission in giant vesicles: direct observation by light microscopy, *J. Am. Chem. Soc.* 114 (1992) 5862–5863.
- [15] D. Needham, D. V. Zhelev, Lysolipid exchange with lipid vesicle membranes, *Ann. Biomed. Eng.* 23 (1995) 287–298.
- [16] T. Tanaka, R. Sano, Y. Yamashita, M. Yamazaki, Shape changes and vesicle fission of giant unilamellar vesicles of liquid-ordered phase membrane induced by lysophosphatidylcholine, *Langmuir* 20 (2004) 9526–9534.

- [17] Y. Inaoka, M. Yamazaki, Vesicle fission of giant unilamellar vesicles of liquid-ordered-phase membranes induced by amphiphiles with a single long hydrocarbon chain, *Langmuir* 23 (2007) 720–728.
- [18] A. Papadopoulos, S. Vehring, I. López-Montero, L. Kutschenko, M. Stöckl, P. F. Devaux, M. Kozlov, T. Pomorski, A. Herrmann, Flip-pase activity detected with unlabeled lipids by shape changes of giant unilamellar vesicles, *J. Biol. Chem.* 282 (21) (2007) 15559–15568.
- [19] R. Wick, M. I. Angelova, P. Walde, P. L. Luisi, Microinjection into giant vesicles and light microscopy investigation of enzyme-mediated vesicle transformations, *Chem. Biol.* 3 (1996) 105–111.
- [20] Y. Tamba, M. Yamazaki, Single giant unilamellar vesicle method reveals effect of antimicrobial peptide magainin 2 on membrane permeability, *Biochemistry* 44 (2005) 15823–15833.
- [21] M. Mally, J. Majhenc, S. Svetina, B. Žekš, The response of giant phospholipid vesicles to pore-forming peptide melittin, *Biochim. Biophys. Acta* 1768 (2007) 1179–1189.
- [22] M. I. Angelova, D. S. Dimitrov, Liposome electroformation, *Faraday Discuss. Chem. Soc.* 81 (1986) 303–311.
- [23] M. I. Angelova, D. S. Dimitrov, A mechanism of liposome electroformation, *Prog. Colloid Polym. Sci.* 76 (1988) 59–67.
- [24] R. C. MacDonald, R. I. MacDonald, B. P. M. Menco, K. Takeshita, N. K. Subbarao, L.-r. Hu, Small-volume extrusion apparatus for preparation of large, unilamellar vesicles, *Biochim. Biophys. Acta* 1061 (1991) 297–303.
- [25] P. Walde, R. Wick, M. Fresta, A. Mangone, P. L. Luisi, Autopoietic self-reproduction of fatty acid vesicles, *J. Am. Chem. Soc.* 116 (1994) 11649–11654.
- [26] I. A. Chen, J. W. Szostak, Membrane growth can generate a transmembrane pH gradient in fatty acid vesicles, *Proc. Natl. Acad. Sci.* 101 (21) (2004) 7965–7970.
- [27] A. Hildebrand, P. Garidel, R. Neubert, A. Blume, Thermodynamics of demicellization of mixed micelles composed of sodium oleate and bile salts, *Langmuir* 20 (2004) 320–328.
- [28] B. J. Frisken, Revisiting the method of cumulants for the analysis of dynamic light-scattering data, *Appl. Opt.* 40 (24) (2001) 4087–4091.
- [29] L. M. S. Loura, F. Fernandes, A. C. Fernandes, J. P. Prates Ramalho, Effects of fluorescent probe NBD-PC on the structure, dynamics and phase transition of DPPC. A molecular dynamics and differential scanning calorimetry study, *Biochim. Biophys. Acta* 1778 (2008) 491–501.
- [30] H. C. Gaede, K. Gawrisch, Lateral diffusion rates of lipid, water, and a hydrophobic drug in a multilamellar liposome, *Biophys. J.* 85 (2003) 1734–1740.
- [31] D. P. Cistola, J. A. Hamilton, D. Jackson, D. M. Small, Ionization and phase behavior of fatty acids in water: application of Gibbs phase rule, *Biochemistry* 27 (1988) 1881–1888.
- [32] H. Fukuda, A. Goto, H. Yoshioka, R. Goto, K. Morigaki, P. Walde, Electron spin resonance study of the pH-induced transformation of micelles to vesicles in an aqueous oleic acid/oleate system, *Langmuir* 17 (2001) 4223–4231.
- [33] M. L. Rogerson, B. H. Robinson, S. Bucak, P. Walde, Kinetic studies of the interaction of fatty acids with phosphatidylcholine vesicles (liposomes), *Colloid. Surf. B* 48 (2006) 24–34.
- [34] J. M. Vanderkooi, J. B. Callis, Pyrene. a probe of lateral diffusion in the hydrophobic region of membranes, *Biochemistry* 13 (19) (1974) 4000–4006.
- [35] M. Almgren, F. Grieser, K. J. Thomas, Dynamic and static aspects of solubilization of neutral arenes in ionic micellar solutions, *J. Am. Chem. Soc.* 101 (2) (1979) 279–291.
- [36] I. A. Chen, J. W. Szostak, A kinetic study of the growth of fatty acid vesicles, *Biophys. J.* 87 (2004) 988–998.
- [37] V. Arrigler, K. Kogej, J. Majhenc, S. Svetina, Interaction of cetylpyridinium chloride with giant lipid vesicles, *Langmuir* 21 (2005) 7653–7661.
- [38] H.-G. Döbereiner, E. Evans, M. Kraus, U. Seifert, M. Wortis, Mapping vesicle shapes into the phase diagram: A comparison of experiment and theory, *Phys. Rev. E* 55 (4) (1997) 4458–4474.
- [39] G. Cevc, D. Marsh, Phospholipid bilayers: Physical principles and models, Vol. 5 of Cell biology, John Wiley and Sons, New York, Chichester, Brisbane, Toronto, Singapore, 1987.
- [40] R. M. Thomas, A. Baici, M. Werder, G. Schulthess, H. Hauser, Kinetics and mechanism of long-chain fatty acid transport into phosphatidylcholine vesicles from various donor systems, *Biochemistry* 41 (2002) 1591–1601.
- [41] A. M. Kleinfeld, P. Chu, C. Romero, Transport of long-chain native fatty acids across lipid bilayer membranes indicates that transbilayer flip-flop is rate-limiting, *Biochemistry* 36 (1997) 14146–14158.
- [42] D. Cupp, J. P. Kampf, A. M. Kleinfeld, Fatty acid-albumin complexes and the determination of the transport of long chain free fatty acids across membranes, *Biochemistry* 43 (2004) 4473–4481.
- [43] F. Kamp, D. Zakim, F. Zhang, N. Noy, J. A. Hamilton, Fatty acid flip-flop in phospholipid bilayers is extremely fast, *Biochemistry* 34 (1995) 11928–11937.
- [44] J. R. Simard, B. K. Pillai, J. A. Hamilton, Fatty acid flip-flop in a model membrane is faster than desorption in the aqueous phase, *Biochemistry* 47 (2008) 9081–9089.
- [45] J. P. Kampf, D. Cupp, A. M. Kleinfeld, Different mechanisms of free fatty acid flip-flop and dissociation revealed by temperature and molecular species dependence of transport across lipid vesicles, *J. Biol. Chem.* 281 (30) (2006) 21566–21574.
- [46] S. Svetina, B. Žekš, The elastic deformability of closed multilayered membranes is the same as that of bilayer membrane, *Eur. Biophys. J.* 21 (1992) 251–255.
- [47] W. Helfrich, Elastic properties of lipid bilayers: Theory and possible experiments, *Z. Naturforsch. C* 28 (1973) 693–703.
- [48] U. Seifert, Configurations of fluid membranes and vesicles, *Adv. Phys.* 46 (1) (1997) 13–137.
- [49] J. Käs, E. Sackmann, Shape transitions and shape stability of giant phospholipid vesicles in pure water induced by area-to-volume change, *Biophys. J.* 60 (1991) 825–844.
- [50] E. Farge, P. F. Devaux, Shape changes of giant liposomes induced by an asymmetric transmembrane distribution of phospholipids, *Biophys. J.* 61 (1992) 347–357.
- [51] J. Israelachvili, Intermolecular and Surface Forces, 2nd Edition, Academic Press, London, San Diego, 1992.
- [52] N. Bergstrand, K. Edwards, Aggregate structure in dilute aqueous dispersions of phospholipids, fatty acids, and lysophospholipids, *Langmuir* 17 (2001) 3245–3253.
- [53] D. V. Zhelev, Exchange of monooleoylphosphatidylcholine with single egg phosphatidylcholine vesicle membranes, *Biophys. J.* 71 (1996) 257–273.
- [54] P. Watson, D. J. Stephens, ER-to-Golgi transport: Form and formation of vesicular and tubular carriers, *Biochim. Biophys. Acta* 1744 (2005) 304–315.
- [55] R. M. Raphael, R. E. Waugh, Accelerated interleaflet transport of phosphatidylcholine molecules in membranes under deformation, *Biophys. J.* 71 (3) (1996) 1374–1388.
- [56] R. M. Raphael, R. E. Waugh, S. Svetina, B. Žekš, Fractional occurrence of defects in membranes and mechanically driven interleaflet phospholipid transport, *Phys. Rev. E* 64 (2001) 051913.
- [57] K. John, S. Schreiber, J. Kubelt, A. Herrmann, P. Müller, Transbilayer movement of phospholipids at the main phase transition of lipid membranes: implications for rapid flip-flop in biological membranes, *Biophys. J.* 83 (6) (2002) 3315–3323.
- [58] J. Liu, J. C. Conboy, 1,2-diacyl-phosphatidylcholine flip-flop measured directly by sum-frequency vibrational spectroscopy, *Biophys. J.* 89 (2005) 2522–2532.